Quantum Electronics **51** (3) 232–239 (2021)

https://doi.org/10.1070/QEL17481

Spectral diagnostics of an optical discharge propagating along a hollow-core optical fibre

I.A. Bufetov, A.N. Kolyadin, Yu.P. Yatsenko, A.F. Kosolapov

Abstract. **The results of spectral diagnostics of an optical discharge (OD) plasma propagating through a hollow-core revolver fibre under the action of repetitively pulsed laser radiation are presented. The revolver fibre is made of silica glass, with a diameter of the hollow core being 20 μm. The peak values of the laser radiation intensity reach 10^{12} W cm^{-2} at an average Nd:YAG laser power of about 2 W. The time-averaged spectrum of the OD plasma in the visible range has the form of a continuum and is close to the blackbody spectrum with a temperature of 13.3–17 kK. The form of the spectrum does not depend on the gas filling of the fibre core (air or argon). In the UV part of the spectrum, lines of neutral silicon are observed, which are indicative of the partial evaporation of the reflecting cladding of the fibre.**

Keywords: *optical discharge, revolver fibre, hollow-core fibre, light detonation.*

1. Introduction

Optical discharges (ODs) were observed earlier in an unlimited volume of gas, beginning with the first report on the air breakdown by *Q*-switched laser radiation [1]. The regimes of OD propagation were investigated both in the form of a light detonation wave (an analogue of a detonation wave in the combustion theory) and in the form of a wave of laser plasma in the "slow burn" regime (an analogue of the heat conduction mechanism of flame propagation through a combustible mixture). The restriction of transverse motion of the OD plasma excited not in free space, but, e.g., in a silica or glass tube, leads to a change in the gas-dynamic propagation conditions and, therefore, to an increase in the OD velocity observed in the slow burn regime from about 20 m s^{-1} to levels comparable to the speed of sound [2]. With an increase in the laser radiation power, a transition of the OD propagation process from the slow burn regime to the light detonation regime can be observed [3]. Note that the propagation of a light detonation wave with restricted transverse expansion of the gas is analogous to the processes occurring in shock tubes and can be used to conduct such studies.

After the appearance of glass optical fibres as a medium for information transmission, as well as for generating laser radiation and realising nonlinear optical effects, the possibility of OD propagation along such fibres was discovered [4, 5]. The observed discharge propagation velocities under the action of continuous laser radiation (~1 m s^{-1}) testify to the heat conduction mechanism of the OD propagation [6]. However, in glass fibres, the OD propagated in a solid (doped silica glass) rather than a gaseous medium. This circumstance excludes a significant effect of the medium motion on the OD parameters, which explains the difference in the observed velocities of the OD propagation in air (~10 m s^{-1} [2]) and in a glass fibre (~1 m s^{-1}). With an increase in the laser radiation intensity in the fibre, a transition was observed from the thermal conduction regime of the OD propagation to the light detonation regime [7].

At the turn of the 20th and 21st centuries, hollow-core fibres (HCFs) appeared [8], which are usually filled with air and only in some cases with other gases at pressures other than atmospheric. HCFs have a nonlinearity that is about three orders of magnitude lower than that of conventional glass fibres, which makes it possible to transmit ultrashort laser pulses through them without distortion over long distances. However, at sufficiently high laser radiation intensities, any fibre, including the HCF, can be destroyed. Relatively recently, the phenomenon of quasi-continuous propagation of the OD along a HCF was discovered under the action of repetitively pulsed laser radiation with an intensity at the maxima of picosecond pulses of about 10^{12} W cm^{-2} and an average power of only ~2 W [9, 10]. This intensity value can be considered close to the threshold for the OD propagation under the action of short pulses. The intensity of cw laser radiation required for the OD propagation in a HCF with a core diameter of 20 μm, estimated using the data [3], is about $5\,5\times10^{8}$ W cm^{-2} [10], which is much greater than the intensity needed for OD propagation in optical fibres with a silica glass core (~1×10^{6} W cm^{-2}). Since HCFs are a kind of a silica glass tube, when planning experiments on the propagation of ODs along them, the results of experiments, similar but performed using much larger setups, can be used [3]. In this case, the use of long waveguides offers new possibilities for studying the processes of shock wave motion along fibres with hypersonic speeds (~300 km s^{-1}) [11] at distances limited only by the available fibre length and the duration of a laser pulse with a power of ~1 MW. For example, when using a laser pulsed setup similar to that described in [12], it is possible to observe the motion of a light detonation wave in a fibre about 1.5 km long for about 5 ms.

The spectral properties of the OD radiation change significantly depending on the conditions of its observation. Figure 1 shows the emission spectra of ODs observed in free space (Fig. 1a) and in a silica glass fibre (Fig. 1b). In the first case, the OD spectrum in air at atmospheric pressure (according to the data of [13, 14]) consists of many individual lines

I.A. Bufetov, A.N. Kolyadin, Yu.P. Yatsenko, A.F. Kosolapov Dianov Fibre Optics Research Centre, Prokhorov General Physics Institute of the Russian Academy of Sciences, ul. Vavilova 38, 119333 Moscow, Russia; e-mail: iabuf@fo.gpi.ru

Received 13 November 2020
Kvantovaya Elektronika **51** (3) 232–239 (2021)
Translated by V.L. Derbov

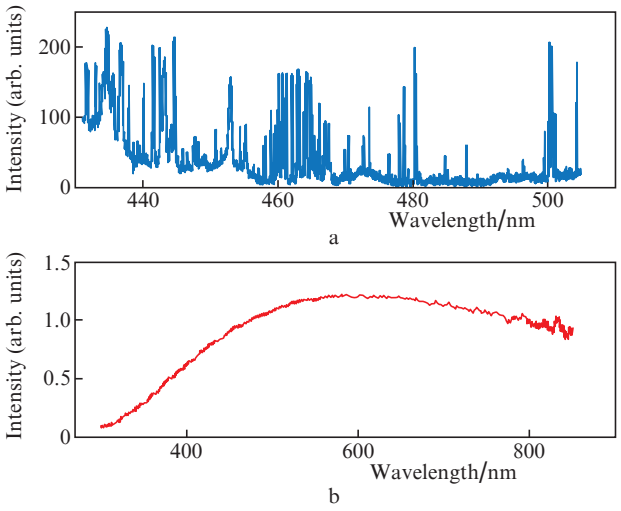

Figure 1. Spectra of an optical discharge in an unlimited volume of air at a pressure of 1 atm (a) and in fibres with a silica glass core (b).

(most of them belonging to singly charged ions and neutral nitrogen and oxygen atoms) observed against the background of a lower-amplitude continuum. In this case, the OD plasma temperature, determined from the intensity ratio of the selected spectral lines, is about 2×10^4 K, and the particle density corresponds to a pressure of 1 atm [13]. In the second case (at significantly higher particle densities), the radiation spectrum of the OD is a continuum without individual spectral lines. Figure 1b shows the spectrum of an OD propagating through an all-solid-state fibre made of silica glass, which was obtained under the action of cw laser radiation with a power of only a few watts [15]. In this case, the OD radiation has a continuous spectrum close to the blackbody radiation. At an intensity of 9 MW cm^{-2} of cw laser radiation in the fibre core, the OD temperature was about 4×10^3 K , and with an increase in intensity to 300 MW cm^{-2}, the temperature increased to 10×10^3 K, while the thermal conductivity of the discharge propagation remained unchanged.

The aim of this work is to study the emission spectra of an optical discharge propagating through a gas-filled hollow-core fibre. Spectra of intrinsic radiation of the OD propagating along the HCF were measured for the first time. The fibre cores were filled with two different gases: air, which can be considered, on average, as a diatomic gas; and argon (a monatomic gas).

2. Experimental setup

We used revolver fibres (RFs) manufactured at the Fibre Optics Research Centre of RAS [16]. Figure 2 shows a cross-section image of such an RF obtained using an electron microscope. The RF was made of F300 silica glass and then covered with a polymer coating (not shown). Eight capillaries fused to the inner surface of the support tube formed the reflective cladding around the hollow core. The RF has the following main geometrical dimensions: the outer diameter of the support tube is 100 μm, the diameter of the hollow core is 20 μm, the inner diameter of the support tube is 36 μm, the capillary wall thickness in the reflective cladding is 0.89 μm, and the wall thickness of the support tube is 32 μm. Since the processes of interaction of laser radiation with the gas and silica glass elements at the core-cladding interface mainly

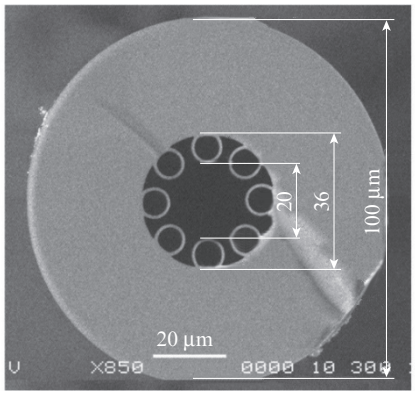

Figure 2. Cross section of the hollow-core revolver fibre used in this work.

affect the plasma formation in a hollow core, the results obtained here are expected highly valid for other types of HCFs.

A schematic of the experiment for observing the propagation of an OD in a fibre filled with air at atmospheric pressure is shown in Fig. 3a. To produce and maintain an OD in the hollow core, we used the repetitively pulsed radiation of a single-mode Nd:YAG laser operating in a combination of *Q*-switched and mode locked regimes. The laser generated nanosecond trains of picosecond pulses with the parameters shown in Fig. 3b. The radiation of the Nd:YAG laser, after being reflected from the spectrally selective mirrors M1 and M2, was coupled through lens L1 into the RF core with an efficiency of up to 80%. The length of the RF segment in all experiments was about 40 cm. At the fibre exit, the average power of laser radiation upon initiation of the OD was about 2 W, the average power of nanosecond pulses was 8 kW, and the maximum power of picosecond pulses reached 1.0 MW. This corresponds to the following intensities of laser radiation on the axis of the fibre core: 5.2×10^9 W cm^{-2} on average in a nanosecond train of pulses and 7.0×10^{11} W cm^{-2} in the maxi-

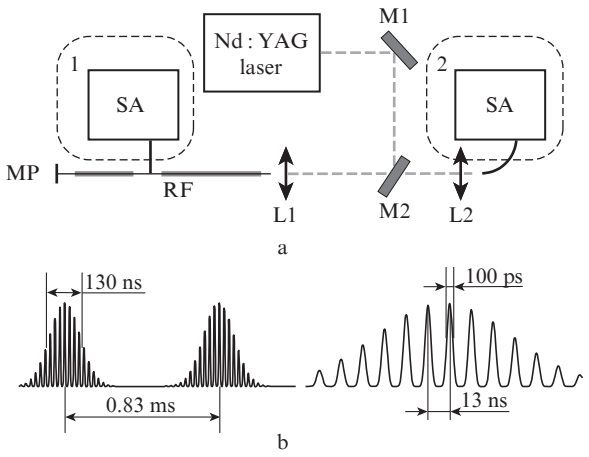

Figure 3. Schematic of the experiment (a) and oscillograms of laser radiation (on the left, nanosecond trains of picosecond pulses; on the right, picosecond pulses, not to scale) (b):
(RF) revolver fibre; (L1, L2) lenses; (M1, M2) mirrors; (SA) spectrum analyser with fibre input; (MP) metal plate for OD initiation. Numbers 1 and 2 mark the positions of the SA in various experiments.

mum of a picosecond pulse. The radiation wavelength of the Nd:YAG laser (λ = 1064 nm) was in the fibre transparency band. The optical loss in the fibre at this wavelength was less than 1 dB m^{-1} and had virtually no effect on the transmission of radiation through the used short segments of the RF. In our experiments, at all available intensities of laser radiation in the fibre core ($\sim 10^{12}$ W cm^{-2}), the OD never appeared spontaneously; therefore, it was initiated using a metal plate, which contacted the output end of the RF (see Fig. 3a).

The RF was coated with a polymer, except for the parts near the ends of the fibre, as well as the area where the OD radiation was launched into the spectrum analyser in position 1 (Fig. 3a). The OD propagation along the fibre in all experiments was recorded using a digital camera at a rate of 240 frames per second, which allowed the OD velocity to be measured as a function of its position or time.

In most previously published papers on spectral diagnostics of ODs, the glow of a discharge itself was observed both perpendicular to the axis of the laser beam (fibre) (see, e.g., [13, 17]), and in the direction of OD propagation along the fibre [15]. We have implemented both of these options. In the experimental scheme, the registration of the OD spectra of emission perpendicular and parallel to the laser beam corresponds to placing the fibre-input optical spectrum analyser (SA) in positions 1 and 2, respectively. In position 1, the spectrum registration is the simplest (on its way to the spectrum analyser, the OD radiation passes only through the silica cladding of the fibre with a thickness of about 30 μm), but at the moments when the OD moves along the fibre, problems arise associated with a relatively low level of the input signal. In position 2 (observation in the direction opposite to the OD motion), the recorded spectrum is largely formed by the optical elements located in the path, including the fibre itself, whose length changes as the OD moves, the lenses L1, L2, and the selectively reflecting mirror M2. All these elements are made of standard K8 optical glass, which absorbs radiation in the UV range. Nevertheless, in experiments with standard all-solid fibres [15], such a scheme looks more preferable because of the virtually unlimited (on a scale of ten seconds) spectrum registration time.

Note that the complex spectrum of optical losses in such fibres significantly affect the results of such measurements in the RF. First, the transmission bands of the fibre (see, e.g., [16] limit the spectrum of the detected radiation passing through the RF. Second, RFs are essentially multimode fibres, and the optical losses of high-order modes significantly exceed the losses of the fundamental mode. It would seem that these problems could be solved by preliminary calibration of the optical path. We calibrated the scheme for recording the OD spectrum using the radiation from a tungsten reference lamp with a known temperature for the initial length of the RF. However, since the OD moves towards the spectrum analyser, the calibration conditions are valid only for the total length of the RF. Therefore, the calibration results were used only for processing the OD spectra obtained approximately during the first 10 ms of the discharge propagation (when the path travelled by the OD is much less than the initial fibre length). This approach was used by us earlier when measuring the temperature of a discharge practically not moving in the RF at radiation intensities close to the threshold values [18].

To carry out experiments on the propagation of ODs in other gases (not in atmospheric air), the fibre should be filled with them at the required pressures. Systems for filling the HCFs with various gases are known (see, e.g., [19]), but they cannot be used directly to initiate a discharge in HCFs, since both ends of the fibre are placed in miniature vacuum chambers, making unavailable the mechanical access to the output end required to initiate OD. To observe the propagation of OD in other gases, we used a scheme in which only the input end of the fibre is located in the vacuum chamber and the output end is directly in the atmosphere (Fig. 4).

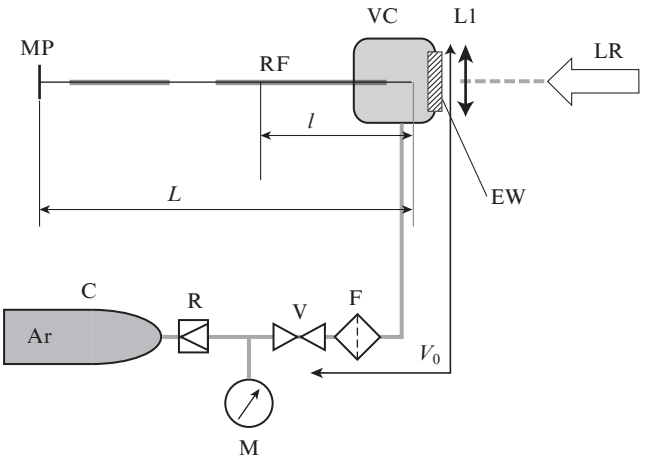

Figure 4. Modified experimental setup (Fig. 3a), providing the possibility of filling the fibre with various gases and initiating the OD: L is the total length of the fibre; l is the current coordinate of the RF section [see Eqns (2) and (3)]; (L1) focusing lens; (LR) laser radiation; (VC) miniature vacuum chamber; (EW) chamber entrance window; (MP) metal plate for OD initiation; (F) mechanical filter; (V) locking valve; (G) pressure gauge; (R) gas pressure reducing regulator; (C) gas cylinder (argon); V_0 is the volume isolated during the experiment from V to VC under pressure P_1.

A miniature vacuum chamber (VC) ~1 cm in size was equipped with a transparent entrance window (EW) for input of laser radiation. The VC was filled with gas (in our case, argon) using an appropriate supply system, including a cylinder (C) with pure argon, a reducing regulator (R), a shut-off valve (V), an additional filter (F) for gas purification, and the necessary connecting pipes. After filling the chamber with argon under pressure P_1, the valve V was closed, and the hermetically isolated volume V_0, including the chamber, the filter F, and the connecting pipes up to the valve V, was connected with the atmosphere only through the hollow core of the RF. Since all channels in the reflecting cladding of the RF have a much smaller diameter, than the hollow core, we neglected their influence. Naturally, a constant gas flow into the atmosphere passes through the RF core, but due to the small diameter of the hollow core (D_c = 20 μm), the flow rate is low. As a result, the RF is filled with the test gas; its output end is in the air, which makes it possible to touch it with the metal plate MP for discharge initiation.

Let us estimate the parameters of a gas flow with a low Reynolds number that is steady in the core of the RF. In this case, the difference in pressure forces performs work mainly against the forces of viscosity (an increase in the kinetic energy of the flowing gas can be neglected) [20], and the flow of an ideal gas in the approximation of a cylindrical capillary is described by the relation [21]

$$N = \frac{(P_1^2 - P_2^2)\pi R^4}{16\mu kTL}, \quad (1)$$

where N is the number of molecules passing per unit time through any cross section of the capillary (independent of the coordinate); μ is the dynamic viscosity factor of the gas; T is the gas temperature; k is the Boltzmann constant; R and L are the capillary radius and length; P_1 is the gas pressure in the VC (3.5 atm in experiments with argon); and P_2 is the gas pressure at the capillary outlet (1 atm).

Using this approximation, it is possible to determine the distributions of the gas velocity $V_{max}(l)$ on the axis of the hollow core and the gas pressure $P(l)$ along the length of the RF. We present for reference the corresponding formulae:

$$V_{max}(l) = \frac{1}{8\mu L}\frac{(P_1^2 - P_2^2)R^2}{\sqrt{P_1^2\left(1 - \frac{l}{L}\right) + P_2^2\frac{l}{L}}}, \quad (2)$$

$$P(l) = \sqrt{P_1^2\left(1 - \frac{l}{L}\right) + P_2^2\frac{l}{L}}. \quad (3)$$

The calculated distributions along the length of the RF of the gas velocity and pressure for the conditions of our experiment are shown in Fig. 5.

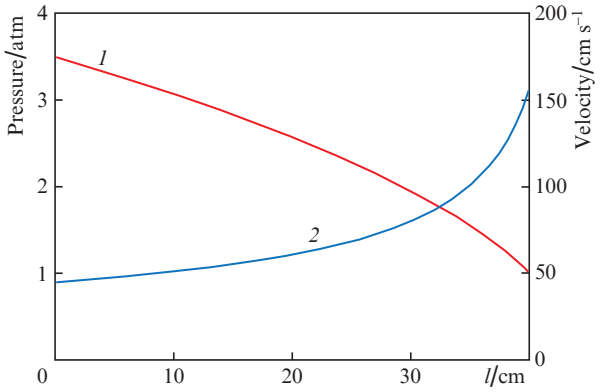

Figure 5. Calculated distributions of pressure (*1*) and gas velocity (*2*) on the RF axis.

The pressure at the inlet to the RF (i.e., in the vacuum chamber) as a function of time is described by the expression

$$P(t) = P_2\frac{1 + [(P_1 - P_2)/(P_1 + P_2)]\exp(-t/\tau)}{1 - [(P_1 - P_2)/(P_1 + P_2)]\exp(-t/\tau)}, \quad (4)$$

where the time constant is

$$\tau = \frac{8\mu V_0 L}{\pi R^4 P_2}. \quad (5)$$

In our experiments, $\tau \approx 4.5 \times 10^5$ s $\approx$ 5.3 days, and the pressure in the volume V_0 decreases very slowly (Fig. 6); therefore, a decrease in pressure in this volume during the preparation of the experiment can be ignored.

Thus, the experiments were carried out at an argon pressure varying along the fibre from 1 to 3.5 atm and a changing velocity of the gas flow counterpropagating with respect to the OD from 1.5 (at the point of discharge initiation) to about 0.5 m s^{-1} (near the point of laser radiation input into the RF).

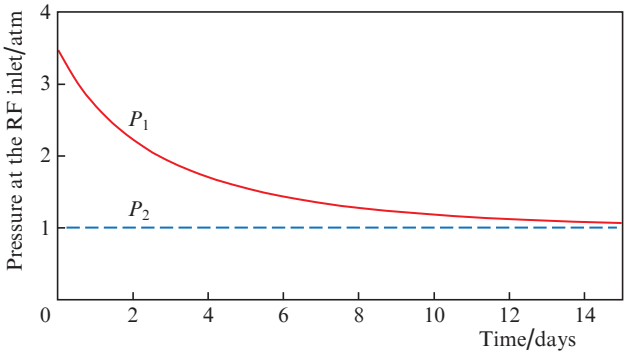

Figure 6. Calculated change in pressure at the RF inlet with time due to gas leakage through the hollow core.

3. Experimental results

3.1. Measurements of the optical discharge motion velocity in air and argon

In the present experiments, as in previous studies [9, 10], after the initiation of an OD in a fibre filled with atmospheric-pressure air, the discharge counterpropagating with respect to the laser radiation with an average velocity of ~1 m s^{-1} was observed. In this case, the velocity of the discharge along the RF, completely covered with a polymer shell, was about 0.75 m s^{-1} (Fig. 7a). An increase in the velocity is observed at the beginning of the propagation of the OD (point 1), when the discharge moves along the segment of the RF without polymer coating (~20 mm long) near the initiation point; here the velocity attains ~1.7 m s^{-1}. Then, upon entering the RF segment coated with polymer (between points 1 and 2), the velocity drops to about 0.75 m s^{-1}. (An explanation of the change in the discharge propagation velocity along the RF in the presence or absence of a polymer coating was proposed in [10].) Further, in the RF segment without a polymer coating (between points 2 and 3), the OD is accelerated again, and its average velocity reaches 2.3 m s^{-1}, and upon passing to the segment of the RF covered with polymer (after point 3), the OD velocity again decreases to 0.75 m s^{-1}. The movement of the discharge along the RF section free from the polymer near the point of laser radiation coupling to the fibre is not shown in Fig. 7a, since the discharge was hidden by the fibre fastening elements.

A somewhat different picture was observed in experiments with a RF filled with argon (Fig. 7b). In this case, before the initiation of the discharge, there was a moving gas in the RF with the initial longitudinal distributions of the velocity and pressure in which are shown in Fig. 5 in contrast to an immobile gas at a pressure of 1 atm in the previous case. The OD initiation in this case did not occur immediately after the appearance of the plasma on the metal plate. In the initial section of the RF (with l not exceeding 10 mm), the movement of the OD (with stops) was observed for ~100 ms, and only after that the propagation of the OD began with an average velocity of ~1 m s^{-1}. No increase in the velocity was observed in the uncoated section of the fibre having a length of ~20 mm (up to mark 1). In the next two sections free of polymer coating, the first, where the spectrum of the OD plasma glow

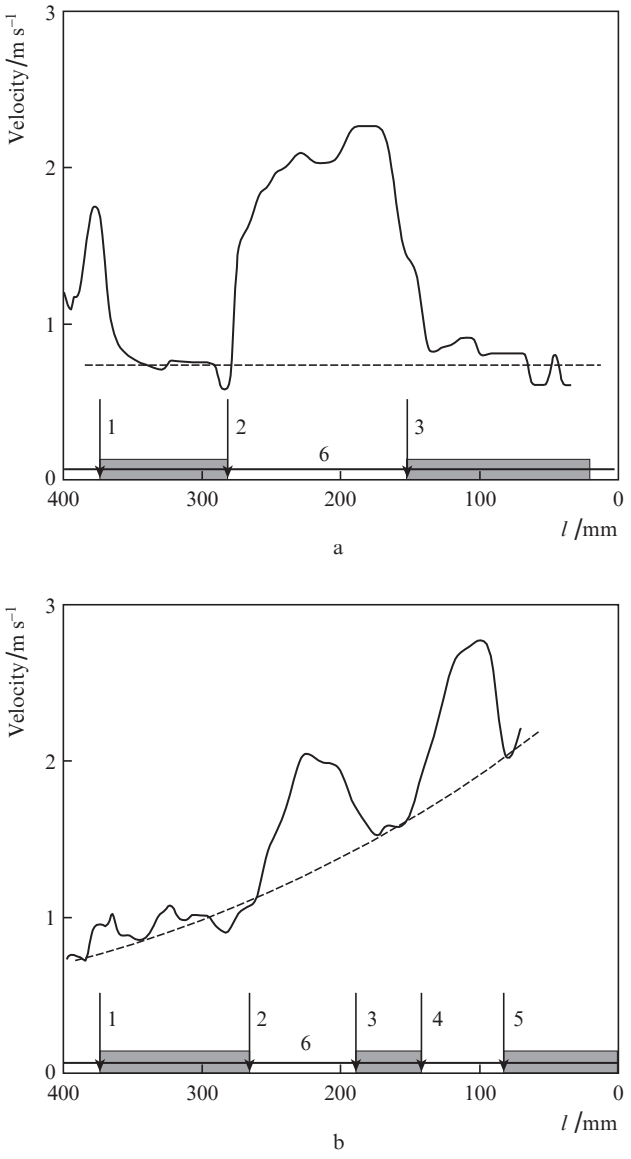

Figure 7. Dependence of the average velocity V of the OD motion on the longitudinal coordinate l of a fibre filled with air (a) and argon (b). Below is a schematic representation of the RF with polymer coated and uncoated parts (6). The dashed line shows the interpolation of the dependence $V(l)$ for the RF completely covered with a polymer.

was recorded, and the second (technological) one, located in front of the place where the RF entered into the glass capillary, a significant increase in the velocity was observed. The capillary with the RF segment glued into it was fixed in the leakproof inlet of the vacuum chamber. Thus, between points 1 and 2, as well as between 3 and 4, the discharge propagated along the RF with a standard polymer coating, and after point 5, along the fibre coated with polymerised glue. In its acoustic properties, the glue is much closer to the standard polymer coating, than air; therefore, this segment of the RF can be considered as having a polymer coating [10]. The dependence of the OD motion average velocity $V(l)$ in a RF completely coated with polymer, shown by a dashed line in Fig. 7b (obtained by interpolation in RF sections without polymer), indicates that $V(l)$ increases from 0.75 m s^{-1} (at the discharge initiation point) to 1.8 m s^{-1} (at point 5 near the VC).

In experiments with the air-filled RF, the average velocity of the OD motion along the fibre without polymer was approximately three times higher than that in the fibre with a polymer coating (Fig. 7a), whereas in the RF filled with argon this difference was significantly less and the velocity increased only by 1.5–1.7 times (Fig. 7b). Undoubtedly, the observed dynamics of the OD motion is affected by a change in the experimental conditions, i.e., replacing a diatomic gas (air) with a monatomic one (argon) and the resulting changes in the adiabatic exponent, pressure and density of the gas, as well as the gas motion with a variable velocity towards the OD. However, rigorous consideration of the effect of all these factors on the motion of the OD against the background of gas-dynamic processes in the discharge itself requires complex calculations that deserve special consideration.

3.2. Spectral measurements of optical discharge radiation

Registration of spectra in the longitudinal direction. The OD plasma emission spectra were recorded by an Ocean Optics 65000 spectrum analyser located in position 2 (Fig. 3a). The instrument could continuously record 25 spectra per second in the wavelength range 0.2–1 μm. During the motion of the OD along a 40 cm-long fibre, approximately 10 emission spectra of the discharge plasma were recorded. Figure 8 shows some of them obtained in one experiment with the RF filled with atmospheric air. Plasma radiation has a continuous spectrum, and it can be assumed that its shape is close to that of the blackbody radiation spectrum.

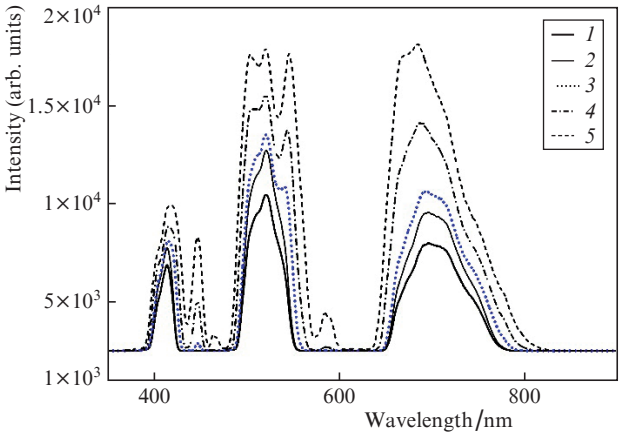

Figure 8. Emission spectra of the optical discharge plasma in the revolver fibre recorded at the time when the OD is located at (*1*) 36, (*2*) 32, (*3*) 16, (*4*) 8, and (*5*) 4 cm from the laser radiation launching point.

The bands of nonzero signal in spectra *1* (l = 36 cm) and *2* (l = 32 cm) (see Fig. 8), correspond to the revolver fibre transparency bands in the range of 300–800 nm, which is limited by the transmission of the deposited layer of the mirror M2 reflecting laser radiation and its glass substrate. As the OD approaches the point, where the laser radiation enters the fibre, the spectra change, and the radiation beyond the transparency band begins to be recorded (spectra 3–5). The sensitivity calibration of the OD spectra recording circuit was carried out prior to the discharge initiation using the radiation of a reference tungsten lamp with an emitting element tempera-

ture of 3110 K, the RF length being $L = 40$ cm. Therefore, to determine the OD plasma temperature we used only spectra *1* and *2* corresponding to the largest values of *l*.

To find out the degree of similarity between the spectra of OD and blackbody radiation, let us use the formula for the blackbody radiation intensity (in W cm^{-2} μm^{-1}):

$$I_\lambda = \varepsilon(\lambda, T) C_1 \lambda^{-5} \frac{1}{\exp(C_2/\lambda T)}, \qquad (6)$$

where $\varepsilon(\lambda, T)$ is the sample emissivity; $C_1 = 2\pi\hbar c^2 = 37418$ W μm^4 cm^{-2}; $C_2 = 2\pi\hbar c/k = 14388$ μm K; λ is the wavelength in microns; k is the Boltzmann constant; and $\hbar$ is Planck's constant.

Figure 9 shows the same spectra *1* and *2* as in Fig. 8, but after correction for the sensitivity of the recording channel and plotted in the Wien coordinates [22]. The fact that a straight line (dashed line in Fig. 9) can approximate the spectrum within the RF transparency bands indicates that the radiation spectrum of the OD itself is close to the blackbody spectrum, the line slope testifies for the OD temperature in the range 16--17.5 kK.

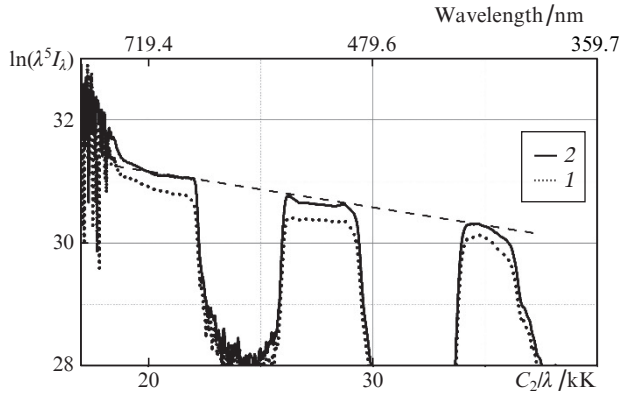

Figure 9. Emission spectra of OD *1* and *2* after calibration of the registration channel with a reference source, plotted in coordinates corresponding to Eqn (6). The dashed line shows the effective slope of the spectrum fragment used for temperature calculation.

Registration of spectra in the direction perpendicular to the RF. Figure 10 shows typical OD plasma emission spectra obtained with the Ocean Optics 2000 spectrum analyser located in position 1 (see Fig. 3a). Spectra *1* and *2* correspond to the OD plasma radiation in experiments with air-filled RF, and spectrum *3*, to an experiment with an RF filled with argon. For ease of comparison, each spectrum has its own amplitude scale. The recording time of the spectra exceeded the time during which the OD moved along the RF; therefore, each of the spectra is a certain averaged characteristic of the OD plasma, containing information about both the hottest and colder regions of the OD. The spectra were obtained without correction for the transmission and sensitivity of the recording channel, since the insufficiently high temperature of the reference lamp (3110 K) made the calibration possible for wavelengths no shorter than 350 nm.

The spectra shown in Fig. 10 differ significantly from the OD spectra in air at atmospheric pressure (see Fig. 1a). They consist of a continuum background, against which in the UV region several clearly distinguished relatively narrow ($(\Delta\lambda \approx 5$ nm) lines a, b, and c are observed. Using the database [23],

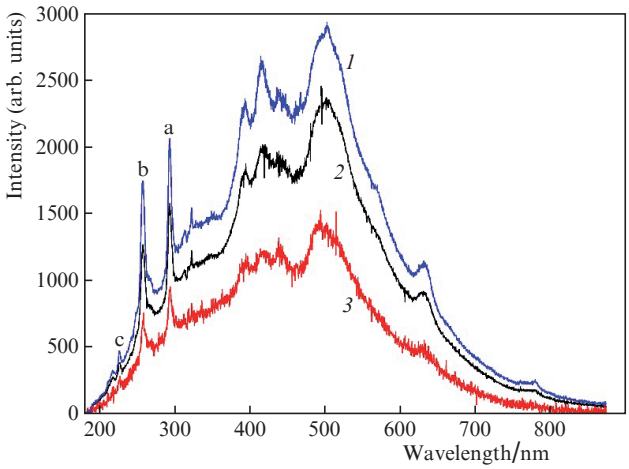

Figure 10. Emission spectra of OD plasma obtained in a fibre filled with air (*1* and *2*) and argon (*3*); a, b and c are spectral lines of neutral silicon atoms.

these lines were identified as emission lines of atomic silicon: line a, $\lambda = 288.1$ nm; b, $\lambda = 251.6$ nm; and c, $\lambda = 221.7$ nm. Estimates made using the same database have shown that, in a low-temperature air plasma ($T \sim 1$ eV) with a small (no greater than 0.1 at.%) silicon impurity, the radiation consists mainly of atomic silicon lines. Lines of other elements that make up the air (oxygen, nitrogen, argon) have luminescence intensities more than two orders of magnitude lower than the luminescence intensity of silicon atoms. The observed lines a, b, and c are the most intense lines of neutral silican in the range 220–300 nm.

The spectrum of the OD plasma in the fibre with atmospheric air obtained after the recording-channel correction using the radiation of a reference tungsten lamp in the range of 350–700 nm is shown in Wien coordinates in Fig. 11 (the initial spectrum *1* in Fig. 10). Since the spectrum shape in this range is close to linear, the spectrum of the OD is close to the blackbody spectrum with the temperature determined by the slope of the straight line. The observed slight deviations of the spectrum from the straight line in the range 360–480 nm can be explained by the deviation of the OD plasma emissivity $\varepsilon(\lambda, T)$ from a constant value in this range (see, e. g., [24]). The spectrum contour for 720–360 nm is approximated by a dashed line, the slope of which allows estimating the average OD plasma temperature as 13.3 kK.

A similar processing of the OD plasma spectrum in an argon-filled fibre (spectrum *3* in Fig. 10) also shows its proximity to the blackbody spectrum. From the slope of the spectrum of OD in argon plotted in the Wien coordinates (Fig. 12) the average plasma temperature was found to be 16 kK.

The closeness of the discharge plasma spectrum, corrected for the sensitivity of the recording channel, and the calculated blackbody spectrum at a temperature of 16 kK in the intensity-wavelength coordinates is shown in the inset to Fig. 12.

Thus, when measured under the same conditions, the temperature of the discharge plasma in the RF filled with air (Fig. 11) turned out to be approximately 20% lower than the temperature of the discharge in argon (Fig. 12). The temperature measured when observing the OD radiation (in air) along the fibre (Fig. 9) was approximately 20% higher than the temperature of the same plasma, determined from its radiation in the direction perpendicular to the fibre (Fig. 11). This circum-

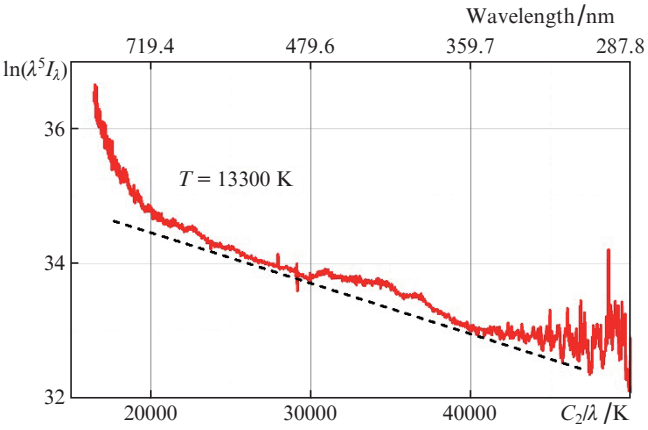

Figure 11. Radiation spectrum of the discharge plasma in an air-filled RF, after calibration of the registration channel with a reference source, plotted in the Wien coordinates. The average OD temperature, determined from the slope of the dashed line, is 13300 K.

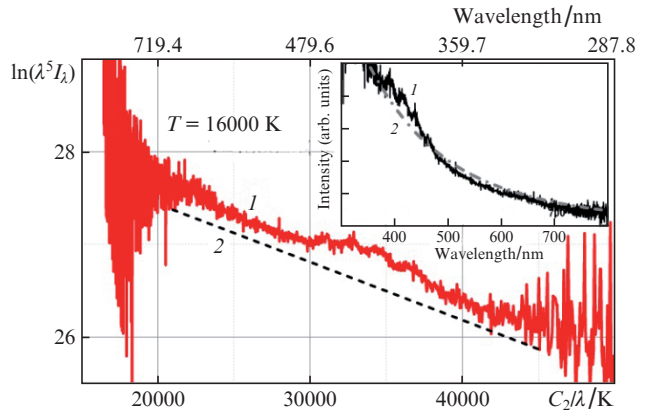

Figure 12. Emission spectrum of the discharge plasma in the RF filled with argon after calibration of the registration channel with a reference source plotted in the Wien coordinates. The average OD temperature is 16000 K. The inset shows the emission spectrum of the OD (*1*) and the emission blackbody spectrum (*2*) at T = 16 kK.

stance can be explained by the fact that, in the latter case, the radiation of colder plasma volumes in the 'tail' of the OD is screened by regions of hotter plasma near the discharge front (as previously noted in Ref. [15]).

4. Conclusions

The spectra of intrinsic emission of an optical discharge propagating along a hollow-core fibre have been measured for the first time. In addition, the propagation of an OD through a hollow fibre filled with argon at a pressure different from atmospheric pressure have been observed for the first time. The discharge was excited by radiation of a repetitively pulsed Nd:YAG laser with a pulse duration of 100 ps and a maximum pulse power of 2 MW.

It was found that the emission spectra of the OD in air and in argon are qualitatively the same (see Fig. 10). The time-averaged emission spectra of OD in the core of a hollow-core fibre filled with air or argon have the form of a continuum and are close to the radiation spectrum of a blackbody with a temperature in the range 13–17 kK. The spectra drastically differ in shape from the nearly line spectrum of the OD in an unlimited volume of gas at atmospheric pressure (Fig. 1a), which indicates a significant pressure increase in the core of a hollow fibre. The observed superposition of several spectral lines of neutral silicon in the UV region on the continuum is, apparently, due to a significant excess of the brightness of these lines over the lines of other elements in the OD in the colder part of the plasma behind the discharge front [23]. The presence of spectral lines belonging to silicon in the OD radiation unambiguously testifies to the partial evaporation of the reflecting cladding elements of the fibre during the passage of the discharge.

The analysis of the OD propagation at a speed of 0.5 to 1.5 m s^{-1} along a fibre filled with argon under a pressure of 1–3.5 atm shows the following. 1) OD can be initiated when the velocity of gas counter flow at the point of initiation exceeds the average velocity of the discharge, since the average OD velocity is determined mainly by the sum of its displacements with velocities of the order of (or greater than) the speed of sound in the gas for short periods of time [10]. 2) As the gas pressure in the fibre core increases, the average propagation velocity of the OD increases. Possibly, this indicates a significant contribution to it from the gas-dynamic component.

The results obtained can be used to design UV radiation sources, as well as devices for protecting fibre systems based on hollow-core fibres, designed to deliver high-power laser radiation, from damage when an optical discharge occurs. In addition, since the propagation velocities of light-detonation (and simply detonation) waves exceeding 100 km s^{-1} [10] are realised when an OD moves along hollow optical fibres [10], the results of this work can also be used to simulate experiments on studying the motion of bodies with high speeds.

Acknowledgements. This work was supported by the Russian Foundation for Basic Research (Research Project No. 18-02-00324).

References

1. Maker P.D., Terhune R.W., Savage C.M., in *Quantum Electronics III*. Ed. by P. Grivet, N. Blombergen (New York: Columbia University Press, 1964) p.1559.
2. Bufetov I.A., Prokhorov A.M., Fedorov V.B., Fomin V.K. *Trudy IOFAN*, **10**, 3 (1988).
3. Bufetov I.A., Fedorov V.B., Fomin V.K. *Combust. Explos. Shock Waves*, **22** (3) 274 (1986) [*Fiz. Goreniya Vzryva*, (3), 18 (1986)].
4. Kashyap R. *Opt. Express*, **21**, 6422 (2013).
5. Hand D.P., Russell P.St.J. *Opt. Lett.*, **13**, 767 (1988).
6. Bufetov I.A., Dianov E.M. *Phys. Usp.*, **48** (1), 91 (2005) [*Usp. Fiz. Nauk*, **175** (1), 100 (2005)].
7. Dianov E.M., Fortov V.E., Bufetov I.A., Efremov V.P., Frolov A.A., Schelev M.Ya., Lozovoy V.I. *JETP Lett.*, **83** (2), 75 (2006) [*Pis'ma Zh. Eksp. Teor. Fiz.*, **83**, 84 (2006)].
8. Cregan R.F., Mangan B.J., Knight J.C., Birks T.A., Russell P.St.J., Roberts P.J., Allan D.C. *Science*, **285**, 1537 (1999).
9. Kolyadin A.N., Kosolapov A.F., Bufetov I.A. *Quantum Electron*, **48**, 1138 (2018) [*Kvantovaya Elektron.*, **48**, 1138 (2018)].
10. Bufetov I.A., Kolyadin A.N., Kosolapov A.F., Efremov V.P., Fortov V.E. *Opt. Express*, **27**, 18296 (2019).
11. Raizer Yu.P. *Laser-Induced Discharge Phenomena* (New York: Consultant Bureau, 1977; Moscow: Nauka, 1974).
12. Bufetov I.A., Fedorov V.B., Fomin V.K. *Kr. Soobshch. Fiz. FIAN*, (10), 21 (1980).
13. Bufetov I.A., Zherdienko V.V., Fedorov V.B., Fomin V.K. *Sov. J. Quantum Electron.*, **16** (9), 1231 (1986) [*Kvantovaya Elektron.*, **13** (9), 1875 (1986)].

14. Fomin V.K. Cand. Diss. (Moscow, IOFAN, 1986).
15. Dianov E.M., Fortov V.E., Bufetov I.A., Efremov V.P., Rakitin A.E., Melkumov M.A., Kulish M.I., Frolov A.A. *IEEE PTL*, **18** (6), 752 (2006).
16. Bufetov I.A., Kosolapov A.F., Pryamikov A.D., Gladyshev A.V., Kolyadin A.N., Krylov A.A., Yatsenko Yu.P., Biriukov A.S. *Fibers*, **6** (2), 39 (2018).
17. Shin-ichi Todoroki. *Japan. J. Appl. Phys.*, **44** (6A), 4022 (2005).
18. Kolyadin A.N., Kosolapov A.F., Yatsenko Yu.P., Bufetov I.A. *Prikl. Fotonika*, **6** (3–4), 171 (2019).
19. Gladyshev A.V., Kolyadin A.N., Kosolapov A.F., Yatsenko Yu.P., Pryamikov A.D., Biryukov A.S., Bufetov I.A., Dianov E.M. *Quantum Electron.*, **45**, 807 (2015) [*Kvantovaya Elektron.*, **45**, 807 (2015)].
20. Prandtl L., Tietjens O.G. *Fundamentals of Hydro- and Aeromechanics* (New York: Dover Publications, 1934).
21. Landau L.D., Lifshits E.M. *Fluid Mechanics* (Oxford: Pergamon Press, 1987; Moscow: Nauka, 1986).
22. Magunov A.N. *Instrum. Exp. Tech.*, **52** (4), 451 (2009) [*Prib. Tekh. Eksp.*, (4), 5 (2009)].
23. Kramida A., Ralchenko Yu., Reader J. NIST ASD Team (2020). NIST Atomic Spectra Database (ver. 5.8); https://physics.nist.gov/asd [2020, November 7]. DOI: https://doi.org/10.18434/T4W30F.
24. Bufetova G.A., Rusanov S.Ya., Seregin V.F., Pyrkov Yu.N., Tsvetkov V.B. *J. Crystal Growth*, **506**, 165 (2019).